https://dx.doi.org/10.21577/0103-5053.20210058

J. Braz. Chem. Soc., Vol. 32, No. 8, 1598-1606, 2021

Article

Preparation of SAPO-34-Based Catalyst for Conversion of Fructose to 5-Hydroxymethylfurfural

Yangyang Zhang,[a] *Chuan Shao,*[a] *Dongling Qin*[a] *and Gang Yang**,[a]

[a]*State Key Laboratory of Materials-Oriented Chemical Engineering, College of Chemical Engineering, Nanjing Tech University, 211800 Nanjing, Jiangsu, China*

Solid acid-catalyzed dehydration of fructose to produce 5-hydroxymethylfurfural (5-HMF) has been a hotspot in biomass conversion research in recent years. In this study, a novel SAPO-34-based catalyst was prepared by consecutive steps of titanium doping, sulfuric acid impregnation, and sulfonic acid functionalization. Characterization of the catalyst with X-ray diffraction (XRD), scanning electron microscopy (SEM), Fourier transform infrared spectroscopy (FTIR), Brunauer-Emmett-Teller (BET), inductively coupled plasma optical emission spectrometer (ICP-OES), and acid-base titration revealed different pore structures and more acid content compared to SAPO-34. The catalyst was applied to the preparation of 5-HMF by dehydration of fructose, and the maximum yield (74.0%) of 5-HMF was obtained by reacting in dimethyl sulfoxide (DMSO) at 170 °C for 50 min. In addition, the applicability of the catalytic system to other substrates and the stability of the catalyst after five cycles were investigated, which are valuable for further probing on the concerned aspects.

Keywords: SAPO-34-based catalyst, fructose, 5-HMF

Introduction

Biomass resources, as an abundant and renewable resource, can be used to produce biofuels, materials, and high value-added chemicals.[1] Among them, selective synthesis of 5-hydroxymethylfurfural (5-HMF) using fructose as the raw materials has been a hot topic in biomass conversion research in recent years.[2] 5-HMF is a high value-added platform compound whose molecular structure consists of an aldehyde group and a hydroxyl group with good chemical reactivity. Fine chemicals, such as medicines,[3] resin plastics,[4] solvents,[5] and biofuels,[6] can be synthesized from 5-HMF through hydrolysis, oxidation, hydrogenation, and other chemical reactions.

So far, inorganic and organic acids,[7,8] ionic liquids,[9] H-form zeolites,[10] etc. have been developed as catalysts for the conversion of carbohydrate into 5-HMF. Among these catalysts, inorganic and organic acids were used as homogeneous catalysts, which offered challenges such as equipment corrosion, difficulty in product separation, and solvent recovery.[11] Ionic liquids can effectively catalyze the dehydration of sugars into 5-HMF; however, its complex preparation process, high cost, and difficulty in product separation limit its application.[12] The limited acidic sites inhibited the 5-HMF yield of the H-form zeolites.[13] Therefore, developing a stable and efficient heterogeneous solid acid catalyst is a promising strategy. The SAPO-34 molecular sieve as a porous zeolite has been a research focus owing to its the high specific surface area, excellent thermal and hydrothermal stabilities, and tunable acidic sites and pore size.[14] Studies concerning SAPO-34 have been widely reported in methanol to olefin (MTO),[15] selective catalytic reduction (SCR),[16] gas adsorption,[17] etc. Yang *et al.*[18] recently synthesized a mesoporous SAPO-34 nanoplate by introducing polyethylene glycol (PEG) as a pore-forming agent to catalyze the formation of 5-HMF from fructose. Zhang *et al.*[19] used SAPO-34 as a catalyst to achieve efficient conversion of glucose in the γ-valerolactone (GVL) solvent. Romo *et al.*[20] reported using a SAPO-34/5A bead catalyst to obtain 45% furfural from xylose and 20% 5-HMF yield from glucose. Sun *et al.*[21] studied that MeSAPOs catalysts prepared from different SAPO zeolites can be used in the reaction of fructose dehydration, indicating that the catalytic activity of zeolite is closely related to its acidity. Chae *et al.*[22] reported the introduction of titanium metal into the SAPO-34 zeolite, and the results indicated that the incorporation of Ti facilitates the formation of Ti (nAl) sites, which generate a negatively

*e-mail: yanggang@njtech.edu.cn

charged framework and increase the concentration of acid centers. In addition, the existence of a hierarchical pore structure and grafting sulfonic acid groups on the catalyst surface can enhance the reaction activity of the catalyst. Dutta *et al.*[23,24] reported that catalysts with a hierarchical pore structure exhibited good catalytic activity for the conversion of carbohydrates to 5-HMF. Karimi *et al.*[25] reported that MCM-41-SO_3H and SBA-15-SO_3H can be used to catalyze the dehydration of fructose. At 140 °C, 5-HMF yields of 59.5 and 69.8% were obtained in a water/methyl isobutyl ketone (MIBK)/2-butanol solvent, respectively. The combination of a mesoporous structure and sulfonic acid groups effectively enhanced the reaction selectivity and catalytic efficiency.

To maximize the potential of the SAPO-34 molecular sieve, we combined the advantages of metal, mesoporous structure, and sulfonic acid group to facilitate fructose dehydration. Based on our team's previous research,[26] in contrast to using SAPO-34 directly as a modified carrier, in this work, we first added titanium atoms to the SAPO-34 molecular sieve framework to form a new catalyst carrier and then performed further modification. We modified the SAPO-34 molecular sieve by doping metal, sulfuric acid impregnation, and grafting sulfonic acid groups to develop a new SAPO-34-based solid acid catalyst and successfully realized effective conversion of fructose and improved yield of 5-HMF.

Experimental

Materials

D-Fructose, 5-HMF, 3-mercaptopropyltrimethoxysilane (MPTMS), inulin, and silica sol were purchased from Aladdin Industrial Co, Ltd. (Shanghai, China). Pseudoboehmite, phosphoric acid, sulfuric acid, hydrogen peroxide (H_2O_2), triethylamine (TEA), sodium chloride, tetrabutyltitanate, dimethyl sulfoxide (DMSO), toluene, D (+)-anhydrous glucose, sucrose, and soluble starch were purchased from Sinopharm Chemical Reagent Co. Ltd. (Shanghai, China). All the chemicals were analytical grade and were used without further purification.

Catalyst preparation

Synthesis of the SAPO-34 molecular sieve

The typical synthetic route of the SAPO-34 molecular sieve is as follows: pseudoboehmite (as the Al source), 85% phosphoric acid (P source), 30% silica sol (Si source), and triethylamine (as a template) were mixed and stirred in a certain order to form a uniform gel solution that has a molar composition of 1.0 Al_2O_3:1.0 P_2O_5:0.6 SiO_2:3.0 TEA:60 H_2O. The gel was transferred to a Teflon-lined stainless steel autoclave and aged at 200 °C for 48 h, followed by filtration, washing with deionized water and drying overnight at 110 °C. Finally, the obtained catalyst was calcined at 550 °C for 6 h to obtain SAPO-34, which was denoted as S-34.

Preparation of TiAPSO-34 molecular sieve

The preparation step was largely similar to the synthesis step of SAPO-34 molecular sieve. Only during the process of the gel preparation, a certain amount of tetrabutyltitanate was added and mixed to obtain the gel. The molar composition of the synthesized gel was as follows: 1.0 Al_2O_3:1.0 P_2O_5:0.6 SiO_2:0.05 TiO_2:3.0 TEA:60 H_2O. The rest of the steps are the same. The obtained catalyst TiAPSO-34 was denoted as TS-34.

Preparation of sulfuric acid-modified TiAPSO-34 molecular sieve

The obtained 1.0 g TiAPSO-34 was impregnated with 10 mL of 0.3 mol L^{-1} sulfuric acid for 1 h, followed by filtration, washing with distilled water, drying at 383 K overnight, and finally calcination at 550 °C for 6 h to obtain the SO_4^{2-}/TiAPSO-34 molecular sieve. It was denoted as STS-34.

Preparation of sulfonated modified SO_4^{2-}/TiAPSO-34 molecular sieve

The sample preparation steps were as follows: 1.0 g of SO_4^{2-}/TiAPSO-34 was accurately weighed into a 100 mL three-necked flask to which 40 mL of anhydrous toluene was added, followed by stirring and refluxing under nitrogen atmosphere for 1 h at 110 °C. Then, 10 mmol of MPTMS was added and refluxing was performed for 24 h. After the reaction was completed, the obtained product was filtered and washed with anhydrous methanol or ethanol several times to remove excess MPTMS. It was dried overnight at 80 °C to obtain SH-SO_4^{2-}/TiAPSO-34. Subsequently, the mixture of SH-SO_4^{2-}/TiAPSO-34 and 30% H_2O_2 solution was stirred at room temperature for 24 h. The product was filtered, washed, and dried at 80 °C for 8 h to obtain SO_3H-SO_4^{2-}/ TiAPSO-34, which was denoted as SO_3H-STS-34. The synthesis route is shown in Scheme 1.

Catalyst characterization

Crystal structures and phase compositions of the catalyst were measured using a Rigaku Miniflex 600 X-ray diffractometer (XRD) with a Cu Kα radiation source at 40 kV, 15 mA (0.02° resolution), and was collected

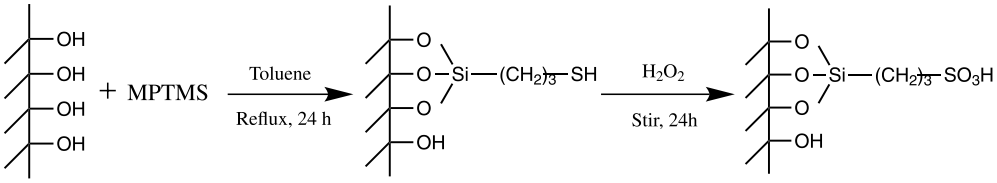

Scheme 1. Synthetic route of SO_3H-STS-34 surface functionalization.

from 5-50° (2θ) at a scanning speed of 10 degree min^{-1}. The morphology and grain size of the catalyst materials were obtained by the Hitachi S-4800 cold field emission scanning electron microscope (SEM). The functional groups of the catalyst samples were determined by the Nicolet Fourier transform infrared (FTIR) spectrometer. Before measurement, the catalyst samples were grounded into fine particles and uniformly mixed with KBr to prepare tablets. Then, spectral analysis was performed in the range of 4000-400 cm^{-1}. The components of various elements in the catalyst were tested and analyzed by the PerkinElmer 7000DV inductively coupled plasma optical emission spectrometer (ICP-OES). The pore volume, pore size, and specific surface area of the catalyst samples were measured by the N_2 adsorption/desorption technique using the Micron ASAP2460 N_2 physical adsorption meter. The acidity of the catalyst was calculated by the acid-base titration method. Then, 50 mg of the catalyst sample was accurately weighed and dispersed in mol L^{-1} NaCl solution and stirred at room temperature for 24 h to perform ion exchange, and then titrated by 0.01 mol L^{-1} NaOH with phenolphthalein as an indicator. The acid density of the catalyst was calculated from the consumed NaOH solution volume.

Catalytic activity test

All reactions were carried out in a dried thick-walled glass reactor, which was heated by an oil-bath. In the experiment, 170 mg of the substrate was dissolved in 10 mL DMSO, and 50 mg of catalyst was added. Then, thick-walled glass reactor was transferred to a preheated oil bath and stirred under a nitrogen atmosphere. After a certain period of reaction at the target temperature, the reactor was immersed in ice water to terminate the reaction in time. Then, the solution was separated by filtration, and the filtrate was diluted for analysis by high performance liquid chromatography (HPLC) with the external standard method.

Determination of products

The quantification and identification of 5-HMF and fructose were conducted by HPLC (Waters 2695) using a photodiode array detector and a refractive index detector, respectively. 5-HMF was measured at 284 nm using XBridge C18 (4.6 × 150 mm × 5 μm) and a photodiode array detector (Waters 2998), and the column temperature was maintained at 303 K. The mobile phase was acetonitrile:water 50:50 (v:v) at a flow rate of 0.8 mL min^{-1}. Fructose was analyzed by XBridge Amide (4.6 × 100 mm × 3.5 μm) and a refractive index detector (Waters 2414), and the column temperature was maintained at 308 K. The mobile phase was acetonitrile:water 78:22 (v:v) at a flow rate of 0.5 mL min^{-1}. The 5-HMF yield, fructose conversion, and 5-HMF selectivity were expressed as follows:

$$\text{Fructose conversion (\%)} = \frac{\text{Moles of fructose reacted}}{\text{Moles of fructose initial}} \times 100 \quad (1)$$

$$\text{5-HMF selectivity (\%)} = \frac{\text{Moles of 5-HMF produced}}{\text{Moles of fructose reacted}} \times 100 \quad (2)$$

$$\text{5-HMF yield (\%)} = \frac{\text{Moles of 5-HMF produced}}{\text{Moles of fructose initial}} \times 100 \quad (3)$$

Results and Discussion

Catalysts characterization

The XRD characterizations of the synthesized S-34, TS-34, STS-34, SO_3H-STS-34 catalysts are shown in Figure 1. All the catalyst samples showed a typical chabazite structure (CHA) with diffraction peaks at 2θ = 9.5, 12.8, 16.0, 20.7, 25.9 and 31.0°.[19] Compared with S-34, with the doping of titanium atoms, the characteristic diffraction peak of TS-34 was strong and sharp, indicating that the heteroatoms in the initial gel resulted in a CHA structure with high crystallinity.[27] The XRD characteristics of STS-34 indicated that its ordering and characteristic peaks were similar to those of the unimpregnated sample (TS-34); however, peak intensities were lower. This means that sulfuric acid has a certain etching effect on the molecular sieve crystals and causes a certain loss of crystallinity.[28] The peak intensity reduction of SO_3H-STS-34 was the most obvious, which may be due to the influence of grafted sulfonic acid groups in the pore channels of the catalyst.[29]

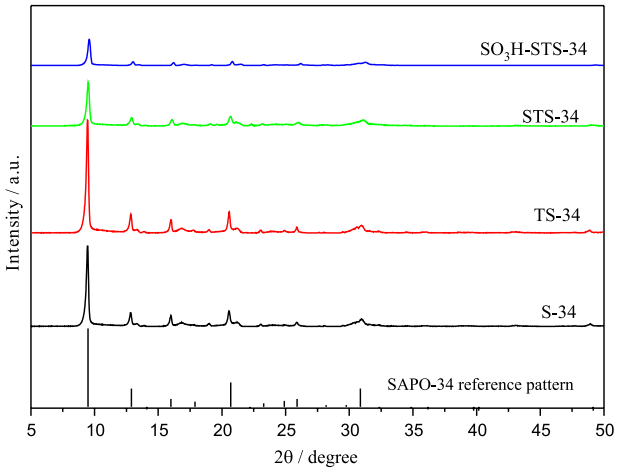

Figure 1. XRD patterns of the different catalysts.

The SEM photographs of the catalysts are shown in Figure 2. The synthesized S-34 possessed a typical SAPO-34 morphology with smooth surface, complete cubic structure, and the average cubic crystal size of 3-7 μm. Compared with the parent S-34, the surface of TS-34 was smoother and showed a complete cubic shape. Moreover, the particle size was smaller, and the cubic crystal size was 2-5 μm. For STS-34, the cubic structure was not destroyed, and a butterfly-like image was formed on the catalyst surface, which was composed of a porous structure obtained by sulfuric acid corrosion. This pattern formation is related to the unique way in which SAPO-34 crystals grow layer by layer from the inside to the outside eight pyramidal subcrystals first form the crystal skeleton; and then grow into cubic crystals by filling the gaps near the center. Therefore, during the acid treatment, the Al element in the butterfly-shaped region that was grown in a later stage was preferentially corroded, and then the unique pattern shown in Figure 2c was formed.[28] The surface of the SO_3H-STS-34 catalyst became very rough after sulfonic acid functionalization. It can be seen that many amorphous substances were attached to surfaces or channels of the catalyst, which confirms the XRD results.

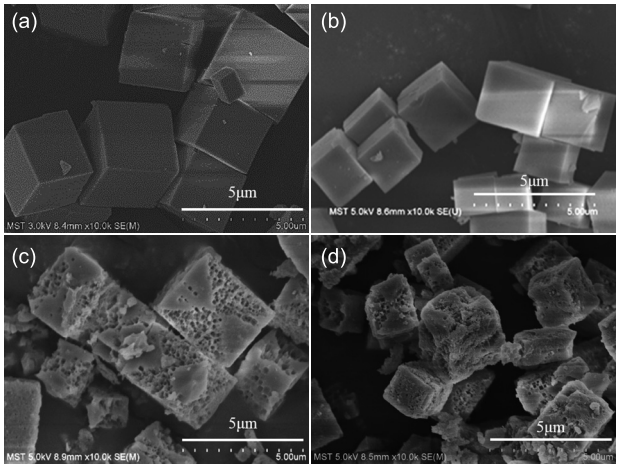

Figure 2. SEM images of (a) S-34, (b) TS-34, (c) STS-34, (d) SO_3H-STS-34.

The FTIR spectra of S-34, TS-34, STS-34, SO_3H-STS-34 are depicted in Figure 3. The bands of approximately 490 cm^{-1} for all the catalysts can be attributed to the TO bending vibration of the TO4 tetrahedron (T = Si, Al, P, and/or Ti). The peaks at 640 and 1090 cm^{-1} are attributed to the D6-ring and Si–O–Si in the SAPO-34 structure, respectively. The bands at 1640 and 3420 cm^{-1} are attributed to the H–O–H bending vibration of the physically adsorbed water molecule and the bridged hydroxyl groups (Si–OH–Al) vibration on the backbone,[22] respectively. Compared with S-34, the bridged hydroxyl peak was higher in TS-34, which indirectly indicated that incorporating S-34 with Ti facilitated the formation of OH groups.[30] In the SO_3H-STS-34 sample, the weak expected peaks at 1480 and 1375 cm^{-1} owing to the C–H deformation vibration peaks of MPTMS.[2] The bands detected at approximately 1152 and 1042 cm^{-1} are assigned to O=S=O and $-SO_3^{2-}$ stretching vibration bands, respectively.[31]

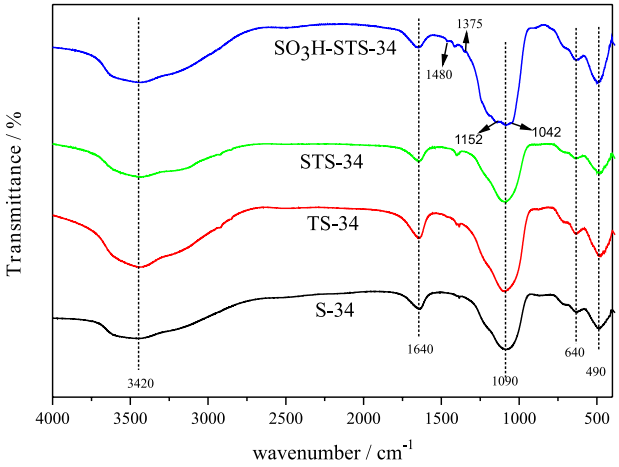

Figure 3. FTIR (KBr) spectra of different catalysts: S-34, TS-34, STS-34, and SO_3H-STS-34.

The textural data, chemical composition, and total acidity of the catalysts are listed in Table 1. Compared with S-34, titanium was incorporated int the framework of TS-34. The acid content increased from 0.78 to 0.93 mmol g^{-1}, indicating that the addition of titanium has a positive effect on the catalyst's acidity. Owing to sulfuric acid corrosion, the pore volumes of STS-34 and SO_3H-STS-34 increased. According to the N_2 adsorption-desorption isotherms of the catalysts in Figure 4, S-34 and TS-34 exhibited the characteristics of a type I isotherm, indicating of the presence of microporous structures in the material. STS-34 and SO_3H-STS-34 exhibited the characteristics

Table 1. Textural data, chemical composition and acidity of the catalysts

Catalyst	S_{BET}[a] / (m^2 g^{-1})	S_{Micro}[b] / (m^2 g^{-1})	Vmeso[c] / (cm^3 g^{-1})	D[b] / nm	Chemical composition				Sulfur contents / %	Acid density / (mmol g^{-1})
					Al	P	Si	Ti		
S-34	536	526	0.02	0.5	0.52	0.50	0.11	0	0.00	0.78
TS-34	569	559	0.02	0.5	0.54	0.41	0.09	0.00073	0.00	0.93
STS-34	632	590	0.10	5.4	0.56	0.43	0.13	0.00063	0.00	0.62
SO_3H-STS-34	460	441	0.05	3.2	0.49	0.38	0.11	0.00133	2.05	1.29

[a]The surface area were calculated by the Brunauer-Emmett-Teller (BET) method; [b]micropore area; [c]mesopore volume; [d]the pore diameters were determined using the Barrett-Joyner-Halenda model.

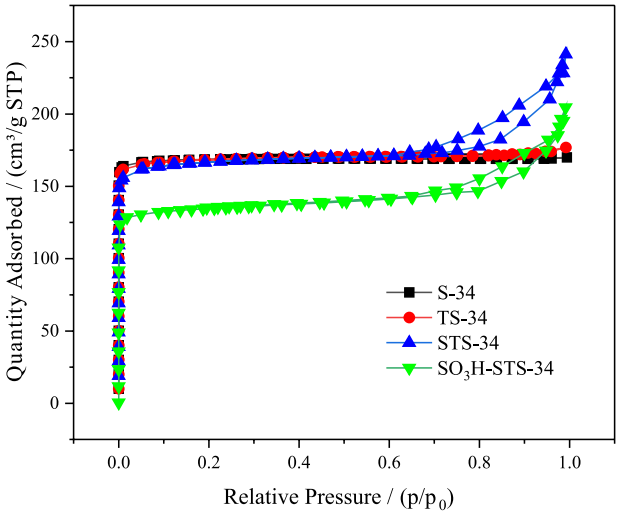

Figure 4. Nitrogen adsorption isotherms of different catalysts: S-34, TS-34, STS-34, and SO_3H-STS-34.

of a type IV isotherm, and the obvious hysteresis loops in the high relative pressure region indicated the presence of mesoporous and macropores structures.[28] After sulfonation modification, the sulfur content in SO_3H-STS-34 increased significantly, and the specific surface area decreased from 632 to 460 m^2 g^{-1}. The acidity increased from 0.62 mmol g^{-1} before sulfonation to 1.29 mmol g^{-1}, which can confirm the successful grafting of the sulfonic acid groups.[32]

D-Fructose dehydration reaction

Effect of different catalysts on fructose dehydration

The effects of S-34, TS-34, STS-34, SO_3H-STS-34 catalysts on fructose dehydration are shown in Figure 5. The maximum 5-HMF yield with S-34 as the catalyst was 35.1%. For TS-34, the maximum 5-HMF yield of 45.6% and selectivity of 46.1% resulted from increased acidity after titanium incorporation. The higher 5-HMF yield of 61.0% and selectivity of 62.2% were acquired using STS-34 as the catalyst. This is because the existence of the mesoporous structure increases the probability of contact between the active sites in the catalyst and fructose; and simultaneously promotes the migration of fructose and 5-HMF in the pores, thereby reducing the resistance to material transfer and inhibiting the occurrence of undesirable side reactions.[33] SO_3H-STS-34 showed the best catalytic effect with a maximum yield and selectivity of 74.0%, which was attributed to the significant increase in the acid content after grafting the sulfonic acid groups and the synergistic effect of mesoporosity.[2] Based on the above discussion, SO_3H-STS-34 was more effective than the other four catalysts in this reaction. Therefore, the optimal reaction conditions were investigated with SO_3H-STS-34 as the target catalyst.

Effect of reaction temperature on fructose dehydration

The effect of reaction temperature on dehydration of fructose into 5-HMF was investigated using SO_3H-STS-34 as the catalyst in the temperature range of 160-190 °C for 100 min. It can be seen from Figure 6 that similar characteristics were observed at various temperatures during the reaction. The yield of 5-HMF increased to the peak value but then decreased with the increasing reaction time. This was attributed to the fact that in addition to the main reaction of fructose dehydration into 5-HMF, there were side reactions as well, including the tandem and/or parallel reactions, and the accumulation of 5-HMF accelerated further degradation of 5-HMF to smaller molecular weight substances, such as levulinic acid and other by-product polymers,[34] as shown in Scheme 2. It was because of these side reactions that significantly high temperatures and long reaction time were not conducive to the stability of 5-HMF. At 160 °C, the maximum yield was only 66.9%, which was mainly because the conversion of fructose was an endothermic reaction, and the lower temperature made it difficult to support the reaction.[29] At 170 °C, the maximum 5-HMF yield was 74.0%. Nevertheless, the highest yield value became lower with increasing temperature (> 170 °C). The reason was that a higher reaction temperature not only supported fructose dehydration to form 5-HMF, but also helped the formation of unknown soluble polymers and insoluble humins.[35] Therefore, 170 °C was the optimal temperature for the reaction.

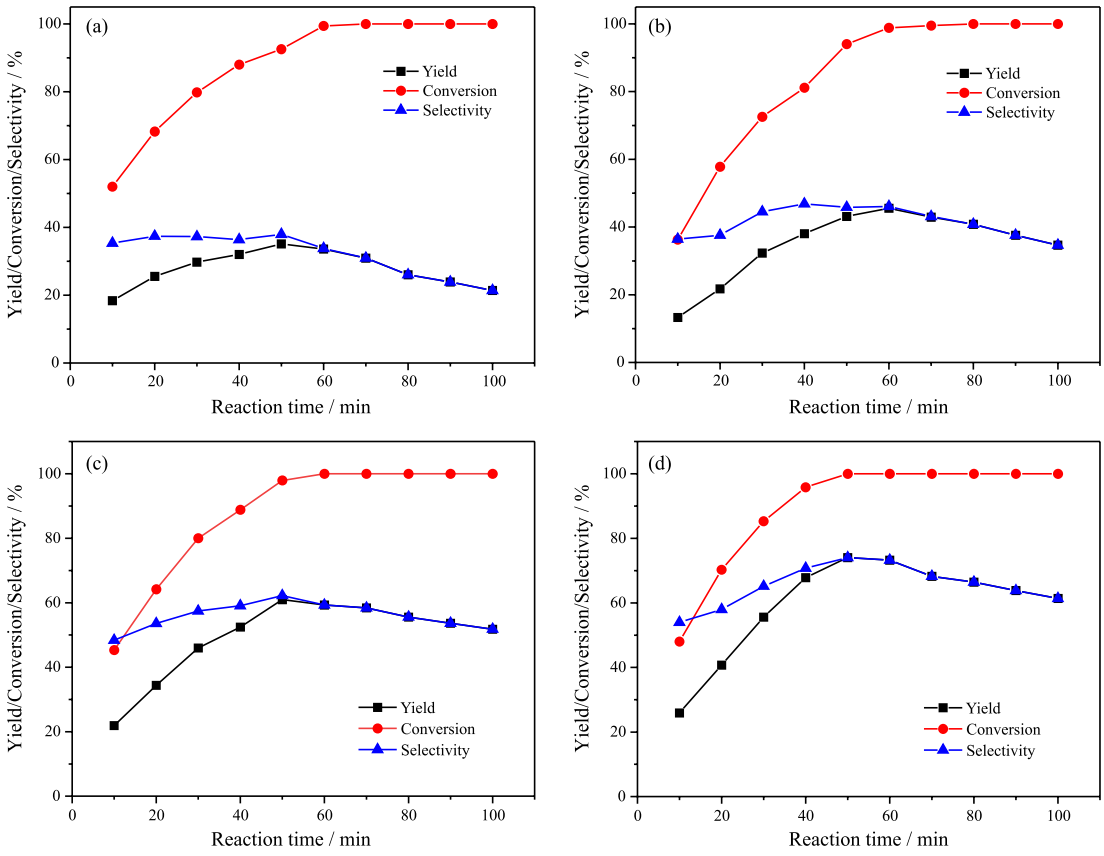

Figure 5. Effect of different catalysts (a) S-34, (b) TS-34, (c) STS-34, and (d) SO_3H-STS-34 on the preparation of 5-HMF by fructose dehydration. Reaction conditions: fructose, 170 mg; catalyst, 50 mg; DMSO, 10 mL; and temperature, 170 °C.

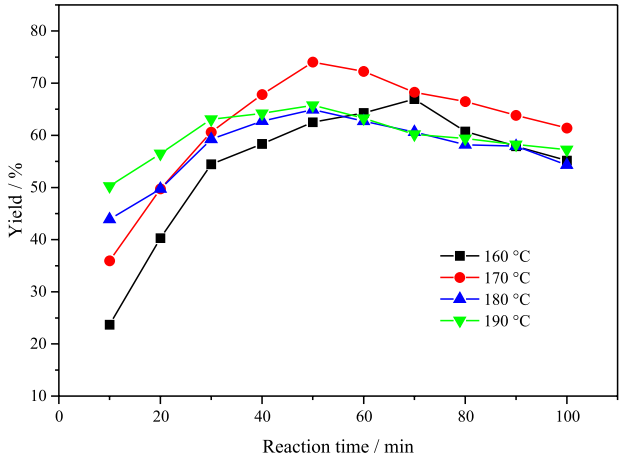

Figure 6. Effect of reaction temperature on the preparation of 5-HMF by fructose dehydration. Reaction conditions: fructose, 170 mg; catalyst, 50 mg; DMSO, 10 mL.

Effect of catalyst dosage on fructose dehydration

The effect of the amount of catalyst on the conversion of fructose to 5-HMF is shown in Figure 7. According to the results shown in Figure 7, fructose can be dehydrated in the DMSO solution with or without the presence of a catalyst; however, utilizing a catalyst can effectively promote the reaction efficiency. When no catalyst was added to the reaction system, a 5-HMF yield of 15.4% and fructose conversion of 35.5% were still obtained. As the catalyst content increased, the number of active sites increased, resulting in a much higher yield and conversion of 5-HMF that those without the catalyst. When the amount of the catalyst reached 50 mg, the highest yield of 5-HMF of 74.0% was obtained, and the fructose was entirely converted. When the amount of catalyst increased to 75 mg, the 5-HMF yield decreased to 61.7%, indicating the oversaturation of the system's acidic sites. A higher amount of catalyst provides more acidic sites, which not only promotes the conversion of fructose but also accelerates the hydration reaction of 5-HMF to generate levulinic acid, formic acid, or other side reactions.[35] Therefore, in the present reaction, a catalyst dose of 50 mg was optimal.

Synthesis of 5-HMF from various substrates

To study the applicability of the catalytic system, a series of experiments were explored considering several sugars as reaction substrates (Table 2). When glucose was used as the substrate, the maximum 5-HMF yield was only 14.9%. When inulin, a polymer in which fructose units are linked by β-1,2 glycosidic bonds,[36] was used as a raw

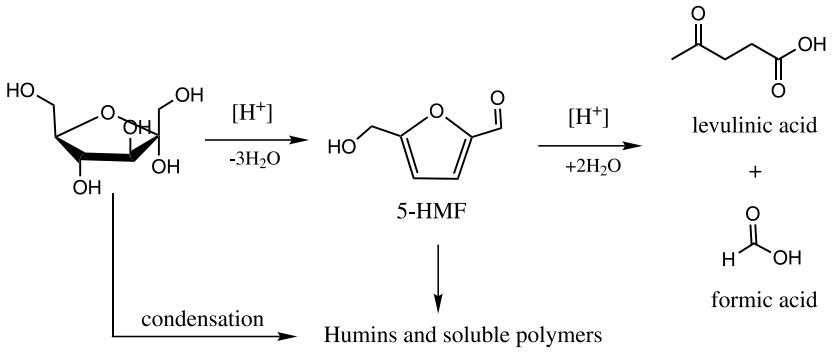

Scheme 2. Reaction pathway of the conversion of fructose to 5-HMF and by-products.

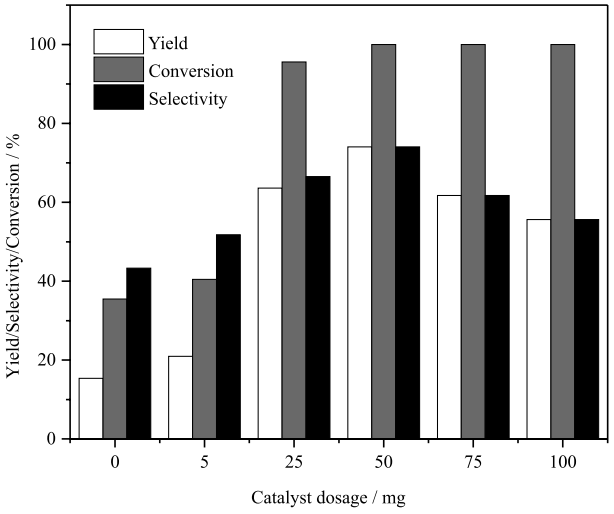

Figure 7. Effect of catalyst dosage on the 5-HMF yield and fructose conversion. Reaction conditions: fructose, 170 mg; DMSO, 10 mL; temperature, 170 °C.

material for the reaction, the 5-HMF yield was 45.6%. Sucrose, when used as the substrate, was hydrolyzed to glucose and fructose, and the yield value was 37.2%. When soluble starch, a polysaccharide composed of glucose units, was used as the substrate, no production of 5-HMF was detected. Therefore, we considered that it is difficult to isomerize glucose to fructose and further dehydrate in the catalytic system. This indicates that the catalytic system has varying degrees of effect on catalyzing other substrates to prepare 5-HMF.

Catalyst cycle test

Catalyst stability is essential for green chemistry and reducing production costs. SO_3H-STS-34, the catalyst with the highest catalytic activity in this study, was chosen to determine the reusability in DMSO. After each reaction, the catalyst was recovered by centrifugation, washed several times with deionized water and ethanol, dried overnight at 110 °C, and reused in the reaction. After five cycles, as shown in Figure 8a, the yield of 5-HMF was still more than 60%. The corresponding fructose conversion rate was above 90%. The catalyst SO_3H-STS-34 was further characterized by XRD and SEM after reusing for five times. As shown in Figures 8b and 8c, the recovered catalyst showed the same peak position as those of a fresh catalyst, which indicated that there was hardly change in the structure of the recovered catalyst, and the catalyst largely maintains a cubic shape. At the same time, the subtle changes in XRD and SEM also reflect the amount of amorphous substances on the recovered catalyst surface reduced, which suggested that the bond cleavage between the sulfonic acid groups and the catalyst support resulted in decreased 5-HMF yield. Therefore, developing a catalyst that minimizes the leaching of sulfonic acid groups is our next research focus. Although there was a slight reduction in the catalytic performance, reusing the catalyst was still effective.

Table 2. 5-HMF synthesis from various substrates in the DMSO system

entry	Substrate	time / min	Temperature / °C	5-HMF yield / %
1	glucose	50	170	7.3
		70	170	12.7
		90	170	14.9
2	inulin	50	170	45.6
		70	170	40.5
		90	170	37.8
3	sucrose	50	170	31.7
		70	170	37.2
		90	170	32.8
4	soluble starch	50	170	ND
		70	170	ND
		90	170	ND

Conditions: substrate, 170 mg; DMSO, 10 mL; SO3H-STS-34,50 mg; reaction time, 100 min. 5-HMF: 5-hydroxymethylfurfural; ND: not detected.

Comparison of different solid acid catalysts with SO_3H-STS-34 catalysts

Table 3 shows the catalytic performances of SO_3H-STS-34 and different reported catalysts for fructose

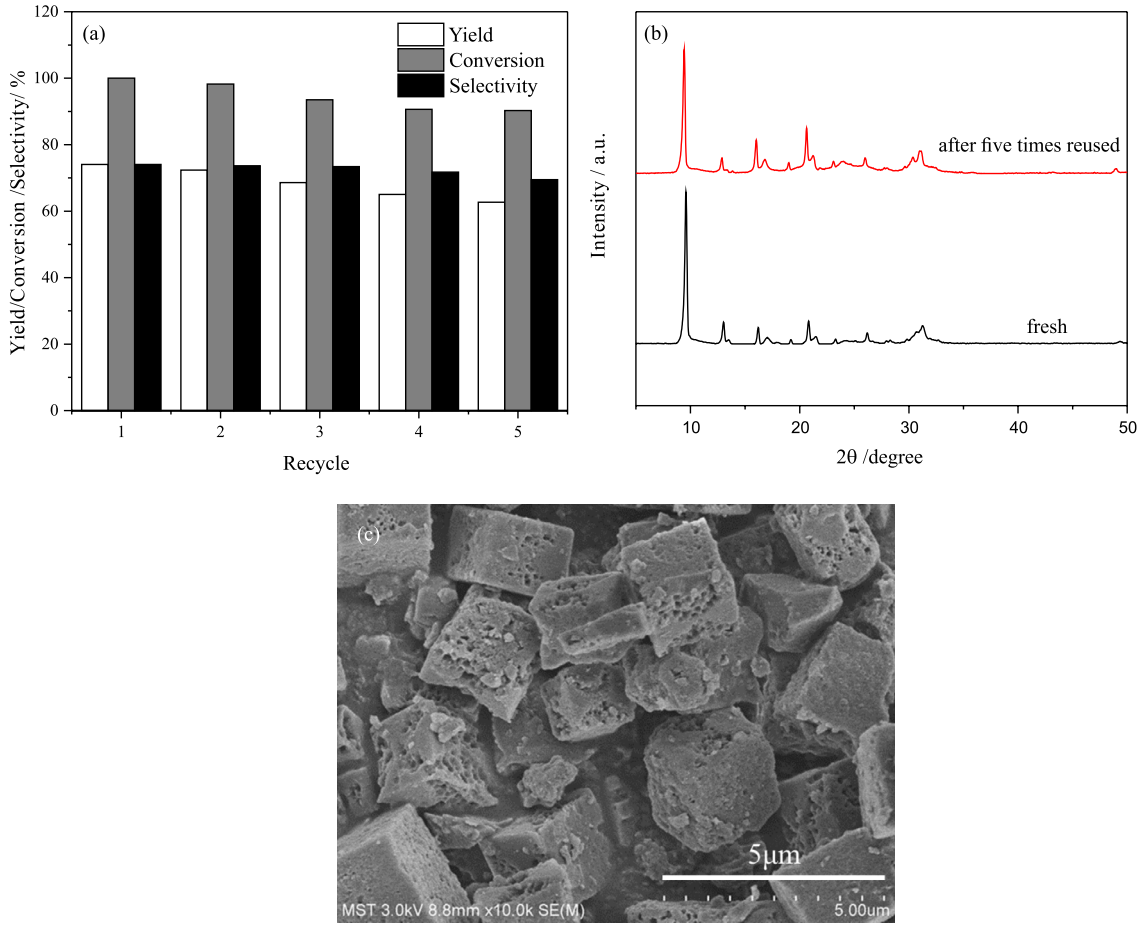

Figure 8. (a) Recyclability of SO_3H-STS-34 in conversion of fructose to 5-HMF, (b) XRD patterns (fresh catalyst and after five times reused), and (c) SEM image (after five times reused).

Table 3. Catalytic performance of different catalysts in the dehydration of fructose

Catalyst	Solvent system	Temperature / °C	Reaction time / min	5-HMF yield / %	Reference
Al-MCM-41	DMSO	165	30	59.4	37
MCM-41-Pr-SO_3H	H_2O/MIBK	140	30	59.5	25
SBA-15-SO_3H	DMSO	135	20	74	38
SBA-15-Pr-SO_3H	THF/H_2O	130	10	12	39
SBA-15-Pr-SO_3H	H_2O/MIBK	140	30	69.8	25
MeSAPO-11	H_2O/DMSO	170	2.5 h	65.1	21
SO_3H-STS-34	DMSO	170	50	74.0	this work

5-HMF: 5-hydroxymethylfurfural; DMSO: dimethyl sulfoxide; MIBK: methyl isobutyl ketone; THF: tetrahydrofuran.

dehydration to 5-HMF conversion in different catalytic systems. It can be seen that SO_3H-STS-34 exhibits certain advantages as a catalyst, which provides an effective strategy for development of new catalysts in the future.

Conclusions

In conclusion, SO_3H-STS-34, which can effectively convert fructose to produce 5-HMF, was successfully prepared by titanium doping, sulfuric acid treatment, and grafting sulfonic acid groups. Compared with the parent S-34, a mesoporous structure was observed in SO_3H-STS-34, and the acidity and yield of 5-HMF were also enhanced significantly. The maximum yield of 5-HMF (74.0%) was obtained in DMSO solution at 170 °C for 50 min. In addition, the catalyst exhibited a certain effect on the dehydration of glucose, sucrose, and inulin. Reusing the catalyst five times indicated that the catalyst maintained a high catalytic performance after regeneration, which provides a new strategy for the development of highly

active and recyclable solid acid catalysts for application in fructose dehydration.

Acknowledgments

The authors acknowledge the facilities support of the National Engineering Research Center for Special Separation Membrane. The authors also thank Qianqian Geng, Zhonghai Liu and Yinzhong Wang for their suggestions and help on this work.

References

1. Arutyunov, V. S.; Lisichkin, G. V.; *Russ. Chem. Rev.* **2017**, *86*, 777.
2. Gan, L.; Lyu, L.; Shen, T.; Wang, S.; *Appl. Catal., A* **2019**, *574*, 132.
3. Ståhlberg, T.; Fu, W.; Woodley, J. M.; Riisager, A.; *ChemSusChem* **2011**, *4*, 451.
4. Siankevich, S.; Savoglidis, G.; Fei, Z.; Laurenczy, G.; Alexander, D. T. L.; Yan, N.; Dyson, P. J.; *J. Catal.* **2014**, *315*, 67.
5. Wettstein, S. G.; Alonso, D. M.; Gürbüz, E. I.; Dumesic, J. A.; *Curr. Opin. Chem. Eng.* **2012**, *1*, 218.
6. Bhaumik, P.; Dhepe, P. L.; *RSC Adv.* **2013**, *3*, 17156.
7. Chheda, J. N.; Roman-Leshkov, Y.; Dumesic, J. A.; *Green Chem.* **2007**, *9*, 342.
8. Salak Asghari, F.; Yoshida, H.; *Ind. Eng. Chem. Res.* **2006**, *45*, 2163.
9. Wang, P.; Yu, H.; Zhan, S.; Wang, S.; *Bioresour. Technol.* **2011**, *102*, 4179.
10. Shi, Y.; Li, X.; Hu, J.; Lu, J.; Ma, Y.; Zhang, Y.; Tang, Y.; *Bioresour. Technol.* **2011**, *21*, 16223.
11. Tang, Y.; Cheng, Y.; Xu, H.; Wang, Y.; Ke, L.; Huang, X.; Liao, X.; Shi, B.; *Catal. Commun.* **2019**, *123*, 96.
12. de Melo, F. C.; Bariviera, W.; Zanchet, L.; de Souza, R. F.; de Souza, M. O.; *Biomass Convers. Biorefin.* **2020**, *10*, 611.
13. Ordomsky, V. V.; Vander Schaaf, J.; Schouten, J. C.; Nijhuis, T. A.; *J. Catal.* **2012**, *287*, 68.
14. Shalmani, F. M.; Halladj, R.; Askari, S.; *RSC Adv.* **2017**, *7*, 26756.
15. Álvaro-Mu Oz, T.; Márquez-álvarez, C.; Sastre, E.; *Appl. Catal., A* **2014**, *472*, 72.
16. Andonova, S.; Tamm, S.; Montreuil, C.; Lambert, C.; Olsson, L.; *Appl. Catal., B* **2016**, *180*, 775.
17. Jie, G.; Wang, C.; Zeng, C.; Zhang, L.; *Microporous Mesoporous Mater.* **2016**, *221*, 128.
18. Yang, H.; Liu, X.; Lu, G.; Wang, Y.; *Microporous Mesoporous Mater.* **2016**, *225*, 144.
19. Zhang, L.; Xi, G.; Chen, Z.; Qi, Z.; Wang, X.; *Chem. Eng. J.* **2017**, *307*, 877.
20. Romo, J. E.; Wu, T.; Huang, X.; Lucero, J.; Irwin, J. L.; Bond, J. Q.; Carreon, M. A.; Wettstein, S. G.; *ACS Omega* **2018**, *3*, 16253.
21. Sun, X.; Wang, J.; Chen, J.; Zheng, J.; Shao, H.; Huang, C.; *Microporous Mesoporous Mater.* **2018**, *259*, 238.
22. Chae, H. J.; Sang, S. P.; Yong, H. S.; Min, B. P.; *Microporous Mesoporous Mater.* **2017**, *259*, 60.
23. Dutta, A.; Gupta, D.; Patra, A. K.; Saha, B.; Bhaumik, A.; *ChemSusChem* **2014**, *7*, 925.
24. Dutta, A.; Patra, A. K.; Dutta, S.; Saha, B.; Bhaumik, A.; *J. Mater. Chem. A* 2**012**, *22*, 14094.
25. Karimi, B.; Mirzaei, H. M.; *RSC Adv.* **2013**, *3*, 20655.
26. Liu, Z.; Sun, Z.; Qin, D.; Yang, G.; *React. Kinet., Mech. Catal.* **2019**, *128*, 523.
27. Zhang, Y.; Ren, Z.; Wang, Y.; Deng, Y.; Li, J.; *Catalysts* **2018**, *8*, 570.
28. Ren, S.; Liu, G.; Wu, X.; Chen, X.; Wu, M.; *Chin. J. Catal.* **2017**, *38*, 123.
29. Saravanamurugan, S.; Sujandi; Prasetyanto, E. A.; Park, S. E.; *Microporous Mesoporous Mater.* **2008**, *112*, 97.
30. Aghaei, E.; Haghighi, M.; Pazhohniya, Z.; Aghamohammadi, S.; *Microporous Mesoporous Mater.* **2016**, *226*, 331.
31. Wataniyakul, P.; Boonnoun, P.; Quitain, A. T.; Sasaki, M.; Kida, T.; Laosiripojana, N.; Shotipruk, A.; *Catal. Commun.* **2017**, *104*, 41.
32. Koujout, S.; Brown, D. R.; *Catal. Lett.* **2004**, *98*, 195.
33. Wang, J.; Zhu, L.; Wang, Y.; Cui, H.; Zhang, Y.; Zhang, Y.; *J. Chem. Technol. Biotechnol.* **2016**, *92*, 1454.
34. Girisuta, B.; Dussan, K.; Haverty, D.; Leahy, J. J.; Hayes, M. H. B.; *Chem. Eng. J.* **2013**, *217*, 61.
35. Hui, S.; Chen, J.; Jing, Z.; Leng, Y.; Wang, J.; *Ind. Eng. Chem. Res.* **2015**, *54*, 1470.
36. Cao, Z.; Fan, Z.; Chen, Y.; Li, M.; Shen, T.; Zhu, C.; Ying, H.; *Appl. Catal., B* **2019**, *244*, 170.
37. Hafizi, H.; Chermahini, A. N.; Saraji, M.; Mohammadnezhad, G.; *Chem. Eng. J.* **2016**, *294*, 380.
38. Bhanja, P.; Modak, A.; Chatterjee, S.; Bhaumik, A.; *ACS Sustainable Chem. Eng.* **2017**, *5*, 2763.
39. Wiedmann, M. K.; Pagan-Torres, Y. J.; Tucker, M. H.; Dumesic, J. A.; Kuech, T. F.; *Mater. Res. Soc. Symp. Proc.* **2011**, *1366*, 11.

Submitted: January 4, 2021
Published online: April 23,2021